Rotational dielectric friction on a generalized charge distribution

D. S. Alavi and D. H. Waldeck

Citation: The Journal of Chemical Physics **94**, 6196 (1991); doi: 10.1063/1.460406
View online: http://dx.doi.org/10.1063/1.460406
View Table of Contents: http://scitation.aip.org/content/aip/journal/jcp/94/9?ver=pdfcov
Published by the AIP Publishing

Rotational dielectric friction on a generalized charge distribution

D. S. Alavi and D. H. Waldeck
Department of Chemistry, University of Pittsburgh, Pittsburgh, Pennsylvania 15260

(Received 1 August 1990; accepted 24 January 1991)

The dielectric friction on a solute molecule reorienting in a liquid solution is computed by modeling the solute as a rigid collection of point charges rotating within a spherical cavity in a dielectric continuum. Such a calculation on an extended charge distribution is a logical progression from existing theories, which treat only single point charges or point dipoles. It is shown how a more realistic charge distribution can change the calculated friction coefficient by several orders of magnitude, and the generalized theory is applied to rotational diffusion data for three phenoxazine dyes in dimethylsulfoxide.

INTRODUCTION

Measurement of solute rotational diffusion times in liquid solution is a sensitive probe of molecular friction. A variety of mechanisms have been proposed to account for this friction including mechanical interactions, long range dielectric interactions, and short range specific solute/solvent interactions.[1] The first two categories are often modeled using theories which treat the solvent as a continuous fluid, ignoring its molecular aspects. The use of hydrodynamics to model the mechanical contribution to the friction is an example of such a continuum theory where the solvent is characterized by its viscosity η. Hydrodynamic theories have been applied with varying degrees of success, working best when the solute molecular volume far exceeds the solvent molecular volume.[1-3]

Dielectric friction may be important for the reorientation of charged or polar solutes in polar solvents, and a number of theories exist to account for the dielectric contribution to the friction.[4-10] Some of these[4-8] are continuum theories in which the solvent is characterized by a frequency dependent dielectric constant $\epsilon(\omega)$, and the friction calculated for a point charge or point dipole reorienting within a spherical cavity in the dielectric. It has recently been shown that most of these theories are inadequate to account for experimentally observed reorientation times, severely underestimating the friction.[11,12]

In particular, we have recently reported rotational reorientation data for three phenoxazine dyes in the polar aprotic solvent dimethylsulfoxide[12] (see Fig. 1). This data was interpreted in terms of various dielectric friction theories.[4-8,10] The semiempirical theory of van der Zwan and Hynes[10] gave the most reasonable agreement with experiment. The theories yielded estimates for dipole moments which were a factor of 5 to 10 too large. It was this failure of continuum theories which motivated the further developments presented in this work.

We begin with the dielectric friction theory of Nee and Zwanzig,[4] which calculates the friction on a point dipole rotating at the center of a cavity within a frequency dependent dielectric. They showed how the frequency dependent dielectric response causes the reaction field of the dipole to lag behind the dipole, exerting a torque which opposes the rotation. We generalize their treatment to a rigid collection of point charges rotating within the cavity. The remainder of this work consists of the following sections. First, the Nee–Zwanzig theory is rederived using the mathematical techniques required for the generalized theory, which is then derived in the following section. Sample calculations on a few simple model systems are presented next, along with application of the new theory to rotational reorientation data for the three phenoxazine dyes discussed above. Lastly, the strengths and weaknesses of the new theory and directions for future work are discussed.

NEE–ZWANZIG THEORY

As an initial step toward the stated goal of this work, we will first derive the result of the Nee–Zwanzig theory for dielectric friction on a point dipole rotating within a spherical cavity in a frequency dependent dielectric continuum. This derivation will serve to illustrate the computational techniques used in treating a more general charge distribution. It should be noted that the method of calculation used here differs from that in the original derivation.[4]

We begin with a point dipole located at the center of a spherical cavity in a continuous dielectric medium. The medium can be completely characterized by a frequency dependent dielectric constant $\epsilon(\omega)$. The first step is to calculate

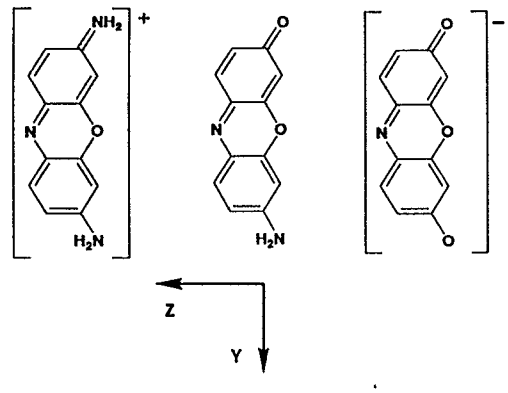

FIG. 1. Molecular structures for the three solute molecules are shown along with the definition of a molecular axis system. The cation is oxazine, the neutral is resorufamine, and the anion is resorufin.

 0021-9606/91/096196-07$03.00

the electrostatic potential inside the cavity with a dipole of moment μ in the $+z$ direction at rest at the center of the cavity. Solution of the Laplace equation[13] for the potential inside and outside the cavity, Φ_{in} and Φ_{out}, can be expressed as a series of Legendre polynomials

$$\Phi_{in}(r,\theta) = \frac{\mu \cos\theta}{r^2} + \sum_{L=0}^{\infty} A_L r^L P_L(\cos\theta), \tag{1}$$

$$\Phi_{out}(r,\theta) = \sum_{L=0}^{\infty} B_L \frac{P_L(\cos\theta)}{r^{L+1}}, \tag{2}$$

where the first term of Eq. (1) is the potential of the dipole and the second is the reaction potential arising from the polarization of the dielectric. The boundary conditions which must be satisfied are

$$\left.\frac{\partial \Phi_{in}}{\partial r}\right|_{r=a} = \epsilon_s \left.\frac{\partial \Phi_{out}}{\partial r}\right|_{r=a}; \quad \left.\frac{\partial \Phi_{in}}{\partial \theta}\right|_{r=a} = \left.\frac{\partial \Phi_{out}}{\partial \theta}\right|_{r=a}, \tag{3}$$

where a is the radius of the cavity and ϵ_s is the static dielectric constant. These boundary conditions force all the A's and B's to be zero except for the $L=1$ terms, which are given by

$$A_1 = \frac{B_1 - \mu}{a^3} = \frac{-2\mu}{a^3}\left(\frac{\epsilon_s - 1}{2\epsilon_s + 1}\right). \tag{4}$$

The negative gradient of the reaction potential is the reaction field **R**, given by

$$\mathbf{R} \equiv \frac{2\mu}{a^3}\left(\frac{\epsilon_s - 1}{2\epsilon_s + 1}\right). \tag{5}$$

Note that in the static case the reaction field and dipole are parallel, and there is no torque exerted on the dipole.

The situation changes when the dipole is allowed to rotate about a perpendicular axis. Because of the frequency dependence of the dielectric constant, the dielectric response of the continuum lags behind any change in applied electric field. If the dipole rotates with angular frequency ω, then the applied electric field at any given point within the dielectric oscillates at ω, with some phase lag we will call $\phi(\omega)$. We can associate this temporal phase angle with a geometrical angle between the dipole μ and the reaction field **R**. The magnitude of the reaction field also changes,[4] which is reflected by the following substitution into Eq. (5):

$$\left(\frac{\epsilon_s - 1}{2\epsilon_s + 1}\right) \rightarrow \left|\frac{\epsilon(\omega) - 1}{2\epsilon(\omega) + 1}\right|. \tag{6}$$

This modification takes into account the change in amplitude of the dielectric response of the medium as a function of frequency. Since the reaction field and the dipole are no longer parallel, there will now be a torque opposing the rotation of the dipole. This torque is the physical basis of energy dissipation, and hence dielectric friction.

The torque **N** exerted on a dipole by an electric field **E** is

$$|\mathbf{N}| = |\boldsymbol{\mu} \times \mathbf{E}| = \mu E \sin\phi. \tag{7}$$

The torque on the rotating dipole is then given by the product of the dipole magnitude, reaction field magnitude, and the sine of the phase lag angle $\phi(\omega)$:

$$\begin{aligned} |\mathbf{N}(\omega)| &= \mu |R(\omega)| \sin\phi(\omega) \\ &= \frac{2\mu^2}{a^3}\left|\frac{\epsilon(\omega) - 1}{2\epsilon(\omega) + 1}\right| \sin\phi(\omega) \\ &= \frac{2\mu^2}{a^3}\left|\mathrm{Im}\left[\frac{\epsilon(\omega) - 1}{2\epsilon(\omega) + 1}\right]\right|. \end{aligned} \tag{8}$$

The frequency dependent friction coefficient $\xi(\omega)$ is defined[4] as the torque divided by the angular frequency ω:

$$\xi(\omega) \equiv \left|\frac{\mathbf{N}(\omega)}{\omega}\right| = \frac{2\mu^2}{a^3}\left|\frac{\mathrm{Im}[(\epsilon(\omega) - 1)/(2\epsilon(\omega) + 1)]}{\omega}\right|. \tag{9}$$

This expression is a general form for the dielectric friction coefficient.

We must now make some assumption as to the form of $\epsilon(\omega)$. The simplest assumption is to assume the dielectric relaxation of the medium can be characterized as a single exponential (Debye relaxation[14]) which leads to the following expression for $\epsilon(\omega)$:

$$\epsilon(\omega) = 1 + \frac{\epsilon_s - 1}{1 + i\omega\tau_D}, \tag{10}$$

where τ_D is the dielectric relaxation time and the high frequency dielectric constant is taken to be one. In the limit of zero frequency we obtain

$$\xi = \lim_{\omega \to 0} \xi(\omega) = \frac{6\mu^2}{a^3}\frac{\epsilon_s - 1}{(2\epsilon_s + 1)^2}\tau_D \tag{11}$$

in agreement with Nee and Zwanzig.[4]

GENERALIZED DIELECTRIC FRICTION THEORY

We will now perform a similar derivation for a rigid collection of point charges. We begin by placing a single stationary point charge q_i at position vector $\mathbf{r}_i$ on the $+z$ axis, and then calculate the electrostatic potential inside a spherical cavity within the dielectric. The charge is inside the cavity, so $r_i \leqslant a$. The electrostatic potential can be written as

$$\Phi_{out}(\mathbf{r}) = \Phi_{out}(r,\theta) = \sum_{L=0}^{\infty} B_L \frac{P_L(\cos\theta)}{r^{L+1}} \tag{12}$$

$$\Phi_{in}(\mathbf{r}) = \Phi_{in}(r,\theta) = \frac{q_i}{|\mathbf{r} - \mathbf{r}_i|} + \sum_{L=0}^{\infty} A_L r^L P_L(\cos\theta). \tag{13}$$

The first term in Eq. (13) represents the potential of the point charge and the second term the reaction potential due to the polarization of the dielectric, which is analogous to the situation described by Eq. (2). The first term can be re-expressed using the identity[13]

$$\frac{1}{|\mathbf{r} - \mathbf{r}_i|} = \sum_{L=0}^{\infty} \frac{r_<^L}{r_>^{L+1}} P_L(\cos\theta)$$

$$r_< \equiv \min(r, r_i), \quad r_> \equiv \max(r, r_i), \tag{14}$$

which allows the potential inside the cavity to be expressed entirely in terms of Legendre polynomials:

$$\Phi_{in}(r,\theta) = \sum_{L=0}^{\infty}\left(A_L r^L + \frac{q_i r_<^L}{r_>^{L+1}}\right) P_L(\cos\theta). \tag{15}$$

We can now use the boundary conditions in Eq. (3) to determine the unknown coefficients in Eqs. (12) and (15), and obtain

$$A_L = \frac{B_L - q_i r_i^L}{a^{2L+1}} = \frac{-q_i r_i^L}{a^{2L+1}} \left[\frac{\epsilon_s - 1}{\epsilon_s + (L/(L+1))} \right], \quad (16)$$

which, in turn, produces the expression for the reaction potential inside the cavity due to the point charge given by

$$\Phi_{rxn}(r,\theta) = \sum_{L=0}^{\infty} \frac{-q_i r_i^L}{a^{2L+1}} \left[\frac{\epsilon_s}{\epsilon_s + (L/(L+1))} \right] \times r^L P_L(\cos\theta). \quad (17)$$

The next step is to generalize Eq. (17) for a collection of N point charges with arbitrary coordinates r_i, θ_i, and ϕ_i. Assuming a linear response of the medium, the principle of superposition can be used to express the reaction field of the charge collection as a sum of terms similar to Eq. (17):

$$\Phi_{rxn}(r,\theta,\phi) = \sum_{i=1}^{N} \sum_{L=0}^{\infty} \frac{-q_i r_i^L}{a^{2L+1}} \left[\frac{\epsilon_s}{\epsilon_s + (L/(L+1))} \right] \times r^L P_L(\cos\gamma_i), \quad (18)$$

where γ_i is the angle between the position vectors $\mathbf{r}$ and $\mathbf{r}_i$. Now we can use the spherical harmonic addition theorem,[13] which states

$$P_L(\cos\gamma_i) = \frac{4\pi}{2L+1} \sum_{M=-L}^{+L} Y^*_{LM}(\theta_i,\phi_i) Y_{LM}(\theta,\phi). \quad (19)$$

Substitution of Eq. (19) into Eq. (18) yields the final expression for the reaction potential of the collection of N point charges:

$$\Phi_{rxn}(r,\theta,\phi) = \sum_{i=1}^{N} \sum_{L=0}^{\infty} \sum_{M=-L}^{L} \frac{-q_i r_i^L}{a^{2L+1}} \left[\frac{\epsilon_s - 1}{\epsilon_s + (L/(L+1))} \right] \times \frac{4\pi}{2L+1} Y^*_{LM}(\theta_i,\phi_i) r^L Y_{LM}(\theta,\phi). \quad (20)$$

Equation (20) gives the reaction field when the charge distribution is stationary. We will now allow the charge distribution to rotate about the z axis at angular frequency ω. This causes the LM th component of the applied electric field to oscillate at $M\omega$, and the magnitude and phase lag of the reaction potential now depend not only on the frequency but also on the indices L and M. This dependence results in a reaction potential that not only lags behind the charge distribution but is also distorted in shape. We can again associate the temporal phase angle with a geometric angle. If the charges are rotating so that the angular velocity vector points in the $+z$ direction, then the torque exerted on q_j by the LM th reaction field component must be computed with the field evaluated at $\phi_j + \phi_L(M\omega)$, where $\phi_L(M\omega)$ is a positive phase angle and is given by

$$\phi_L(M\omega) = \left| \text{phase} \left[\frac{\epsilon(M\omega) - 1}{\epsilon(M\omega) + (L/(L+1))} \right] \right|, \quad (21)$$

and with the field magnitude scaled by the substitution

$$\left[\frac{\epsilon_s - 1}{\epsilon_s + (L/(L+1))} \right] \rightarrow \left| \frac{\epsilon(M\omega) - 1}{\epsilon(M\omega) + (L/(L+1))} \right|. \quad (22)$$

The friction from the LM th component of the reaction potential as the charge distribution rotates about the z axis is

$$\xi_{LM}(\omega) \equiv -\frac{[N_Z(\omega)]_{LM}}{\omega_z} = \sum_{j=1}^{N} \frac{q_j r_j \sin\theta_j}{\omega} \times \{E_\phi[r_j,\theta_j,\phi_j + \phi_L(M\omega)]\}_{LM}, \quad (23)$$

where E_ϕ is the component of the reaction field in the ϕ direction, and is defined as

$$E_\phi \equiv \frac{-1}{r\sin\theta} \frac{\partial \Phi_{rxn}}{\partial \phi}. \quad (24)$$

Substitutions of Eqs. (22) into (20), (20) into (24), and (24) into (23), followed by summation over L and M yields a general expression for the dielectric friction coefficient for rotation about the z axis:

$$\xi(\omega) = \sum_{j=1}^{N} \sum_{i=1}^{N} \sum_{L=0}^{\infty} \sum_{M=-L}^{L} \frac{-q_i q_j}{a\omega} \left(\frac{r_i}{a} \right)^L \left(\frac{r_j}{a} \right)^L \times \left| \frac{\epsilon(M\omega) - 1}{\epsilon(M\omega) + (L/(L+1))} \right| \frac{4\pi}{2L+1} iMY^*_{LM}(\theta_i,\phi_i) \times Y_{LM}[\theta_j,\phi_j + \phi_L(M\omega)], \quad (25)$$

where $\phi_L(\omega)$ is given by Eq. (21).

Equation (25) is the full expression for the dielectric friction experienced by the rotating charge distribution. We will now make some assumptions regarding the behavior of the dielectric and some approximations in the evaluation of Eq. (25) in order to obtain an expression similar to the Nee–Zwanzig result [Eq. (11)]. First of all, since we will be going to the limit of zero frequency, we can treat the lag angle from Eq. (21) as small. In this limit, we can write[13]

$$\sum_{M=-L}^{L} iMY^*_{LM}(\theta_i,\phi_i) Y_{LM}[\theta_j,\phi_j + \phi_L(M\omega)]$$

$$\approx \sum_{M=-L}^{L} iMY^*_{LM}(\theta_i,\phi_i)[Y_{LM}(\theta_j,\phi_j) + iM\phi_L(M\omega) Y_{LM}(\theta_j,\phi_j)]$$

$$= \sum_{M=-L}^{L} Y^*_{LM}(\theta_i,\phi_i) Y_{LM}(\theta_j,\phi_j)[iM - M^2\phi_L(M\omega)]$$

$$= \cdots = \sum_{M=1}^{L} -2 \frac{2L+1}{4\pi} \frac{(L-M)!}{(L+M)!} P_L^M(\cos\theta_i) P_L^M(\cos\theta_j)[M\sin M\phi_{ji} + M^2\phi_L(M\omega)\cos M\phi_{ji}], \quad (26)$$

where $\phi_{ji} = \phi_j - \phi_i$. When Eq. (26) is substituted into Eq. (25), the double sum over i and j causes the sin $M\phi_{ji}$ term to cancel out, and the expression for the friction becomes

$$\xi(\omega) \approx \sum_{j=1}^{N}\sum_{i=1}^{N}\sum_{L=1}^{\infty}\sum_{M=1}^{L} \frac{2q_iq_j}{a}\left(\frac{r_i}{a}\right)^L\left(\frac{r_j}{a}\right)^L \times\left|\frac{\epsilon(M\omega)-1}{\epsilon(M\omega)+(L/(L+1))}\right|\frac{\phi_L(M\omega)}{\omega} \times M^2\frac{(L-M)!}{(L+M)!}\cos M\phi_{ji}P_L^M(\cos\theta_i)P_L^M(\cos\theta_j). \tag{27}$$

Since $\phi_L(M\omega)$ is small, we can write

$$\left|\frac{\epsilon(M\omega)-1}{\epsilon(M\omega)+(L/(L+1))}\right|\phi_L(M\omega) \approx\left|\mathrm{Im}\left[\frac{\epsilon(M\omega)-1}{\epsilon(M\omega)+(L/(L+1))}\right]\right|. \tag{28}$$

If we further assume Eq. (10) for the behavior of $\epsilon(\omega)$ (Debye relaxation), and go to the limit of zero frequency, then

$$\frac{1}{\omega}\left|\mathrm{Im}\left[\frac{\epsilon(M\omega)-1}{\epsilon(M\omega)+(L/(L+1))}\right]\right| \to\left(\frac{2L+1}{L+1}\right)\frac{\epsilon_s-1}{[\epsilon_s+(L/(L+1))]^2}M\tau_D. \tag{29}$$

One final approximation is required to obtain an expression similar to Eq. (11). The expression $[\epsilon_s + (L/(L+1))]$ in the denominator of Eq. (29) has values ranging from $[\epsilon_s + 1/2]$ for $L = 1$ up to $[\epsilon_s + 1]$ for large L. For polar solvents with fairly large dielectric constants ($\epsilon_s \geqslant 10$), the change is $\leqslant 5\%$. Furthermore, the terms of higher L become progressively smaller due to their dependence on $(r_i/a)^L$ and $(r_j/a)^L$. So it seems reasonable to replace $[\epsilon_s + (L/L+1)]$ with $[\epsilon_s + 1/2]$. Doing so yields the final form for the dielectric friction coefficient for rotation about the z axis:

$$\xi = \frac{8}{a}\frac{(\epsilon_s-1)}{(2\epsilon_s+1)^2}\tau_D \times\sum_{j=1}^{N}\sum_{i=1}^{N}\sum_{L=1}^{\infty}\sum_{M=1}^{L}\left(\frac{2L+1}{L+1}\right)\frac{(L-M)!}{(L+M)!}M^3 \times q_iq_j\left(\frac{r_i}{a}\right)^L\left(\frac{r_j}{a}\right)^L P_L^M(\cos\theta_i)P_L^M(\cos\theta_j)\cos M\phi_{ji}. \tag{30}$$

The expression for the friction has the same dependence on the dielectric properties of the solvent as the Nee–Zwanzig expression [Eq. (11)], but a very different dependence on the electrical properties of the solute. In fact, the $L = 1$ term in Eq. (30) is nearly the same as the Nee–Zwanzig result, with μ^2 replaced by $\mu_x^2 + \mu_y^2$ for rotation about the z axis. We now show that the higher order terms neglected by the assumption of a point dipole can be quite significant, and cannot, in general, be neglected.

RESULTS AND DISCUSSION

Some sample calculations were performed on two simple model systems to illustrate the quantitative differences between the calculated friction coefficients for point dipoles and extended charge distributions. Equation (30) was evaluated numerically using the ASYST scientific software package on a personal computer. For each M value, P_M^M and P_{M+1}^M were evaluated explicitly[15] as

$$P_M^M(x) = \frac{(1-x^2)^{M/2}}{2^M}\frac{(2M)!}{M!}$$

$$P_{M+1}^M(x) = \frac{(1-x^2)^{M/2}}{2^{M+1}}\frac{(2M+2)!}{(M+1)!}x. \tag{31}$$

The remaining L terms were computed using the recurrence relation[15]

$$P_{L+1}^M(x) = \frac{(2L+1)xP_L^M(x) - (L+M)P_{L-1}^M(x)}{(L-M+1)}. \tag{32}$$

After computation of the friction about the z axis, computation of the friction about the other two axes was done by simply relabeling the coordinate axes and repeating the computation.

TABLE I. Friction on a neutral dipole. ($\mu = 4.8$ D, $a = 5$ Å).

q (e)	r (Å)	r/a	$\left(\frac{\xi(2\epsilon_s+1)^2}{\tau_D(\epsilon_s-1)}\right)$ 10^{-12} erg	ξ/ξ_{NZ}	Minimum L for $\leqslant 5\%$ error
∞	0.0	0.0	1.105	1.0	1
1.0	0.5	0.1	1.108	1.003	1
0.4	1.25	0.25	1.194	1.081	3
0.2	2.5	0.5	2.930	2.652	5
0.133	3.75	0.75	35.98	32.56	13
0.121	4.125	0.825	141.5	128.1	19
0.111	4.5	0.9	1253	1134	33

The first model system is a dipole consisting of two point charges $+q$ and $-q$ located at $\pm r$ on the x axis, which would model a neutral polar molecule. The values of q and r were varied so that $\mu = 2qr$ was constant and equal to 4.8 D. This dipole was placed in a cavity of radius $a = 5$ Å, and the friction was calculated for rotation about the z axis. The numerical results are shown in Table I. It is apparent that the ratio r/a is extremely important in determining the friction experienced by the rotating dipole. For $r/a \leqslant 0.25$, the point dipole expression [Eq. (11)] accounts for the friction well. For $r/a = 0.5$, however, the point dipole expression underestimates the friction by more than a factor of 2. Two additional terms in the full expression [Eq. (30)] are enough to account for the friction (to within 5%). (In this case all the even terms are zero.) The differences are more dramatic as r/a increases beyond 0.5. When $r/a = 0.75$, terms up to $L = 13$ are required and the point dipole expression is more than a factor of 30 too small, and $r/a = 0.9$ requires $L = 33$ and produces over a 1000-fold increase in friction over the case of a point dipole.

The second test system studied was a single point charge $q = 1e$ at $x = r$, with the friction calculated for rotation about z within a 5 Å cavity. This sort of charge distribution has frequently been used to model polyatomic ions with a charge localized on one atomic center.[11,16] The numerical

TABLE II. Friction on an ion. ($q = 1$ e, $a = 5$ Å).

μ (D)	r (Å)	r/a	$\left(\frac{\xi(2\epsilon_s+1)^2}{\tau_D(\epsilon_s-1)}\right)$ (10^{-12} erg)	$\left(\frac{\xi_{NZ}(2\epsilon_s+1)^2}{\tau_D(\epsilon_s-1)}\right)$ (10^{-12} erg)	ξ/ξ_{NZ}	Minimum L for <5% error
0.0	0.0	0.0	0.0	0.0	NA	NA
2.4	0.5	0.1	0.2954	0.2764	1.068	2
6.0	1.25	0.25	2.605	1.728	1.508	3
12.0	2.5	0.5	35.81	6.912	5.181	5
18.0	3.75	0.75	1014	15.55	65.21	12
19.8	4.125	0.825	4819	18.81	256.2	18
21.6	4.5	0.9	50880	22.39	2272	34

results are in listed in Table II. Once again it is apparent that the ratio r/a is very important. The point dipole expression assumes $\mu = qr$, and is adequate for $r/a \lesssim 0.1$, but as r/a increases, the friction calculated by Eq. (30) exceeds that of a point dipole by a factor of over 2200 for $r/a = 0.9$. The maximum L value required to compute the friction also increases rapidly, from 3 for $r/a = 0.25$ to 34 for $r/a = 0.9$.

The reason for this sensitivity to r/a is clear from Eq. (30), which looks like a geometric series in $(r/a)^2$. The error resulting from truncation of such a series after L terms is $(r/a)^{2L}$. The series in Eq. (30) also has angular terms which increase with L, so the actual number of terms required to achieve a given level of accuracy is actually somewhat more than for the simple geometric series. The physical basis for this sensitivity can also be easily understood. The electric field of a point charge varies as $1/r^2$, so the strength of the electric field polarizing the dielectric increases dramatically as the charge is brought closer to the boundary of the cavity. This, in turn, increases the degree of coupling between the dielectric and the moving charge, resulting in a larger torque, and hence a larger friction coefficient. It is clear that when calculating dielectric friction for a molecule in liquid solution, replacing the actual charge distribution by a point charge or point dipole located at the center of the molecule can lead to significant underestimation of the friction. It is the amount of charge "close" to the boundary of the cavity which is of primary importance in producing dielectric friction.

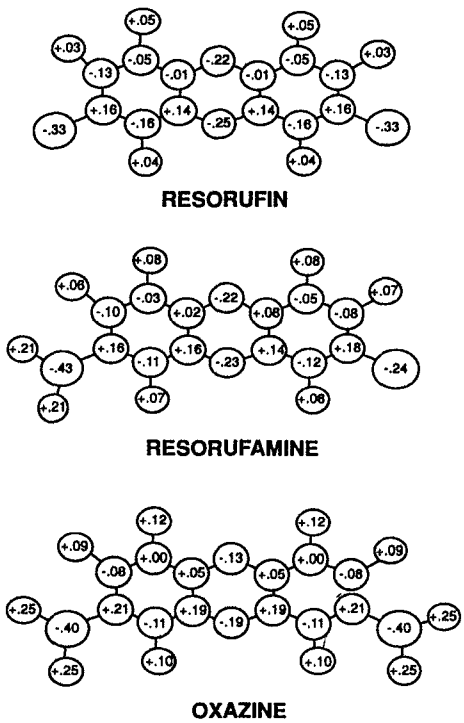

FIG. 2. Shown are ball and stick models of the solute molecules with the partial charge of each atom indicated.

The general expression for dielectric friction was applied to the rotational diffusion of three phenoxazine dyes in liquid solution (Fig. 1). We recently reported experimental results for rotational diffusion of these dyes in the polar aprotic solvent dimethylsulfoxide (DMSO).[12] Figure 2 shows partial charges localized on each atomic center. These charges were obtained from electronic structure calculations performed on the departmental FPS 500 computer using the GAUSSIAN 86 software package. A Hartree–Fock self-consistent field calculation was performed, and the partial charges shown in Fig. 2 are the Mulliken charges calculated for each atomic center in the molecule. The molecule was then modeled as a rigid collection of point charges using these Mulliken charges, and three dielectric friction coefficients were calculated using Eq. (30). As noted above, the friction coefficient becomes very sensitive to the cavity radius for $r/a \gtrsim 0.75$. We therefore calculated the dielectric friction coefficient required to reproduce our experimental results for reorientation times (τ_{OR}), and then chose a cavity radius which produced the correct friction coefficient.

The calculation of the required dielectric friction coefficient was performed as follows. The calculations showed that the friction about the two shorter axes (x and z) of the molecules are much larger than about the long axis (y). Since the transition moment points along the long axis, the friction about the other two axes predominantly determines the experimentally observed reorientation time (see the Appendix). Hydrodynamic friction coefficients were calculated for each axis using a slip boundary condition assuming the molecule is an ellipsoid with axial radii of 6.5, 3.5, and 2.0 Å [2d]. It was found empirically that the solvent viscosity η is roughly proportional to $[(\epsilon_S - 1)\tau_D]/[(2\epsilon_S + 1)^2]$, and a least squares fit yielded a proportionality constant of

1.99×10^{11} erg/cm^3. In this way both the hydrodynamic and dielectric components of the friction could be related to a single solvent parameter. The reorientation time was then calculated from the diffusion constants D_x and D_z as follows:

$$\tau_{OR}\approx\frac{1}{3(D_x+D_z)}=\frac{1}{3kT[(1/\xi_x)+(1/\xi_z)]}$$
$$=\frac{1}{3kT[(1/(\xi_{x,HYD}+\xi_{x,DF}))+(1/(\xi_{z,HYD}+\xi_{Z,DF}))]}, \tag{33}$$

but

$$\xi_{HYD}=A\eta\approx AC\frac{\epsilon_s-1}{(2\epsilon_s+1)^2}\tau_D \tag{34}$$

and

$$\xi_{DF}=B\frac{\epsilon_s-1}{(2\epsilon_s+1)^2}\tau_D \tag{35}$$

so substitution of Eqs. (34) and (35) into Eq. (33) yields

$$\tau_{OR}\approx\frac{\epsilon_s-1}{(2\epsilon_s+1)^2}\frac{\tau_D}{T}$$
$$\times\frac{1}{3k[(1/(A_xC+B_x))+(1/(A_zC+B_z))]}. \tag{36}$$

Fitting the experimental data yields a slope for τ_{OR} vs $[(\epsilon_S-1)\tau_D]/[(2\epsilon_S+1)^2T]$. The experimental fitting parameters are given in Table III. This experimentally obtained slope can be compared to Eq. (36), and the slope can be written in terms of the friction coefficients

$$3k(\text{slope})=\frac{1}{[(1/(A_xC+B_x))+(1/(A_zC+B_z))]}. \tag{37}$$

If we assume $B_x\approx B_z\approx B$, then Eq. (37) results in a quadratic equation for B, the coefficients of which depend on the known quantities A_x, A_z, C, k, and the experimental slope. After solving for B, a radius is found which produces B_x and B_z, which are close to the calculated value of B. The results of this procedure are summarized in Table IV. The cavity radii obtained are all physically reasonable, and very close to the largest axial radius of 6.5 Å used for the hydrodynamic calculation. These results would seem to indicate that Eq. (30) gives a reasonable estimate of the dielectric friction on these solute molecules as they reorient in DMSO. As seen earlier, the primary factor determining the friction is the amount of charge located close to the cavity boundary. In the specific case of these three phenoxazine dyes, the addition of hydrogen atoms on the functional groups at the ends of the molecules places more charge near the cavity boundary, and hence increases the dielectric friction. This explains the qualitative trend that oxazine (four amino hydrogens) reorients more slowly than resorufamine (two hydrogens), which, in turn, reorients more slowly than resorufin (no hydrogens). This concept was verified by changing the charge on the amino hydrogens while keeping the total charge of the amino group constant. This observation underscores the sensitivity of the friction not only to the cavity radius chosen but also to the charge distribution near the cavity boundary.

TABLE III. Experimental fitting parameters for τ_{OR} vs $[(\epsilon_s-1)\tau_D]/[(2\epsilon_s+1)^2T]$.

Solute	Slope (10^4 K)	Intercept (ps)
Resorufin	28.07 ± 0.92	-8.1 ± 1.7
Resorufamine	47.90 ± 4.33	-9.3 ± 8.4
Oxazine	85.23 ± 2.81	-19.6 ± 5.4

A further refinement of the theory developed here would be the use of an elliptical cavity, which would more realistically model the solute molecule's environment. A change in the cavity geometry changes the size and position dependence of the reaction potential, which will affect the calculation of the friction. The charges near the center of the molecule would be closer to the boundary of an elliptical cavity, increasing their contribution to the friction, and possibly leading to better agreement between the cavity dimensions and the dimensions used for the hydrodynamic calculation. Unfortunately, solution of the Laplace equation is much more difficult in elliptical coordinates, and displacement of the dielectric continuum by rotation of the nonspherical particle will complicate the calculation. Further work is being pursued in this area.

While Eq. (30) is reasonably successful in reproducing experimentally observed reorientation times, the extreme sensitivity of the friction to the cavity radius is troubling. One can produce a wide range of friction coefficients, even

TABLE IV. Calculation of friction coefficients Note: $C=1.99\times10^{11}$ erg/cm^3.

Solute	AC (10^{-12} erg)	B (10^{-12} erg) (quad)	Radius (Å)	B (10^{-12} erg) [Eq. (30)]	ξ_{DF}/ξ_{HYD}	Maximum r/a
Resorufin	x: 84	94	6.75	x: 98.7	x: 1.18	0.728
	y: 43			y: 2.6	y: 0.06	
	z: 239			z: 90.5	z: 0.38	
Resorufamine	x: 84	249	6.50	x: 262	x: 3.12	0.841
	y: 43			y: 7.6	y: 0.18	
	z: 239			z: 242	z: 1.01	
Oxazine	x: 84	553	6.71	x: 464	x: 5.53	0.849
	y: 43			y: 7.6	y: 0.18	
	z: 239			z: 657	z: 2.75	

invert the order of the three solutes studied here, with small changes in the cavity radius. Since the expression diverges as the charges are brought close to the boundary, in a sense one could obtain any desired value for the friction coefficient. This sensitivity may be representative of the inappropriateness of continuum models to molecular systems where a well defined cavity boundary generally cannot be determined. Modification of the theory to allow for dependence of the dielectric constant on wave vector as well as frequency may alleviate this divergence problem, reducing the contributions of large L terms in which the reaction potential varies on length scales comparable to or smaller than the solvent molecule size.

CONCLUSIONS

A continuum theory for rotational dielectric friction has been developed which accounts for the charge distribution of the solute in a more realistic way than previous theories. Where the earlier theories modeled the solute's charge distribution with a single point charge or point dipole at the center of the molecule, the theory developed here models the solute as a rigid collection of point charges rotating within a spherical cavity within a dielectric continuum. This increases the calculated friction, and brings the theory into reasonable agreement with experimentally obtained reorientation times.

Unfortunately, the friction calculated using Eq. (30) is extremely sensitive to the cavity radius when there are charges located near the cavity boundary. This sensitivity may be an indication that the use of continuum based theories is not appropriate on molecular length scales. In addition, the use of a spherical cavity is not always an appropriate choice for the solute molecule shape, and development of the theory for an elliptical cavity and for a wave vector as well as frequency dependent dielectric constant is being pursued. Nevertheless, the theory presented here represents a significant improvement over earlier theories of dielectric friction.

ACKNOWLEDGMENTS

This work was supported with funds from National Science Foundation Grant No. CHE-8613468. We thank P. E. Siska for helpful discussions and suggestions regarding the numerical evaluation of Eq. (30), and M. Falcetta and K. D. Jordan for assistance with the GAUSSIAN program.

APPENDIX

The reorientation time τ_{OR} is defined as the decay time of the orientational anisotropy $r(t)$. If the solute has diffusion constants D_x, D_y, and D_z, has a transition moment pointing along the y axis, and has $D_y > D_x$ or D_z, then $r(t)$ can be written as[1]

$$r(t) = \left[\frac{1}{2} + \frac{3(D - D_y)}{4\Delta}\right]\exp[-(6D + 2\Delta)t] + \left[\frac{1}{2} - \frac{3(D - D_y)}{4\Delta}\right]\exp[-(6D - 2\Delta)t]$$

where

$$D \equiv (D_x + D_y + D_z)/3$$

and

$$\Delta \equiv (D_x^2 + D_y^2 + D_z^2 - D_xD_y - D_yD_z - D_xD_z)^{1/2}.$$

If we define

$$\bar{D} \equiv (D_x + D_z)/2, \quad y \equiv \frac{D_x}{\bar{D}}, \quad \text{and} \quad x \equiv \frac{D_y}{\bar{D}},$$

then we obtain

$$r(t) = \frac{3}{2}\left(\frac{y-1}{x-1}\right)^2 \exp\left\{-6\bar{D}t\left[\frac{2x-1}{3} + \frac{(y-1)^2}{x-1}\right]\right\} + \left[1 - \frac{3}{2}\left[\frac{y-1}{x-1}\right]^2\right] \times \exp\left\{-6\bar{D}t\left[1 + \frac{(y-1)^2}{x-1}\right]\right\}$$

if $(y-1)/(x-1)$ is small. In this limit it is clear that the first term decays rapidly and has a small amplitude, and the overall decay is dominated by the second term. The reorientation time can then be expressed as $\tau_{OR} = 1/6\bar{D}$, as was assumed in the derivation of Eq. (37).

[1] G. R. Fleming, *Chemical Applications of Ultrafast Spectroscopy* (Oxford, New York, 1986).
[2] (a) A. Einstein, *Investigations on the Theory of the Brownian Movement* (Dover, New York, 1956); (b) E. W. Small and C. Isenberg, Biopolymers **16**, 1907 (1977); (c) C. M. Hu and R. Zwanzig, J. Chem. Phys. **60**, 4363 (1974); (d) G. K. Youngren and A. Acrivos, *ibid.* **63**, 3846 (1975); (e) J. L. Dote, D. Kivelson and R. N. Schwartz, J. Phys. Chem. **85**, 2169 (1981).
[3] (a) D. Ben-Amotz and J. M. Drake, J. Chem. Phys. **89**, 1019 (1988); (b) D. Ben-Amotz and T. W. Scott, *ibid.* **87**, 3739 (1987); (c) R. Zwanzig, *ibid.* **68**, 4325 (1978); (d) J. O'Dell and B. J. Berne, *ibid.* **63**, 2376 (1975); (e) J. T. Hynes, R. Kapral, and M. Weinberg, Chem. Phys. Lett. **47**, 575 (1977).
[4] T. W. Nee and R. Zwanzig, J. Chem. Phys. **52**, 6353 (1970).
[5] J. B. Hubbard and P. G. Wolynes, J. Chem. Phys. **69**, 998 (1978).
[6] J. B. Hubbard, J. Chem. Phys. **69**, 1007 (1978).
[7] (a) B. U. Felderhof, Mol. Phys. **48**, 1269 (1983); (b) **48**, 1283 (1983); (c) E. Nowak, J. Chem. Phys. **79**, 976 (1983).
[8] P. G. Wolynes, Annu. Rev. Phys. Chem. **31**, 345 (1980).
[9] P. Madden and D. Kivelson, J. Phys. Chem. **86**, 4244 (1982).
[10] G. van der Zwan and J. T. Hynes, J. Phys. Chem. **89**, 4181 (1985).
[11] J. D. Simon and P. A. Thompson, J. Chem. Phys. **92**, 2891 (1990).
[12] (a) D. S. Alavi, R. S. Hartman, and D. H. Waldeck, *Ultrafast Phenomena VII*, edited by C. B. Harris, E. Ippen, G. A. Mourou, and A. H. Zewan (Springer, Berlin, 1990), pp. 450–452 (b) D. S. Alavi, R. S. Hartman and D. H. Waldeck, J. Chem. Phys. (in press).
[13] J. D. Jackson, *Classical Electrodynamics* 2nd ed. (Wiley, New York, 1975).
[14] C. J. F. Böttcher, *Theory of Electric Polarization* (Elsevier, New York, 1973).
[15] A. R. Edmonds, *Angular Momentum in Quantum Mechanics* (Princeton University, Princeton, 1957).
[16] (a) L. A. Phillips, S. P. Webb, and J. H. Clark, J. Chem. Phys. **83**, 5810 (1985); (b) E. F. Gudgin Templeton and G. A. Kenney-Wallace, J. Phys. Chem. **90**, 2896 (1986); (c) **90**, 5441 (1986); (d) E. F. Gudgin Templeton, E. L. Quitevis, and G. A. Kenney-Wallace, *ibid.* **89**, 3238 (1985); (e) D. Kivelson and K. G. Spears, *ibid.* **89**, 1999 (1985).